

# Spin-Peierls transition in $\text{TiPO}_4$

J.M. Law, C. Hoch, and R.K. Kremer

The complex interplay between charge, orbital, spin and lattice degrees of freedom in low-dimensional systems with pronounced quantum fluctuations allows for a plethora of complex and unusual ground states. Most of the prominent examples of low-dimensional quantum antiferromagnets with exotic ground states contain  $\text{Cu}^{2+}$  ( $3d^9$ ,  $S = 1/2$ ) ions with one hole present in the  $e_g$  orbitals. Compounds of early transition-metal elements with one electron in the  $d$  shell are less frequently investigated. With a  $3d^1$  electron in a high-symmetry or slightly distorted octahedral environment, the orbital degeneracy of the  $t_{2g}$  states opens new degrees of freedom, with the prospect of low-energy orbital excitations and the interesting possibility of destabilization of coherent spin/orbital ordering by quantum fluctuations.  $3d^1$  systems can be realized in compounds containing, e.g.,  $\text{Ti}^{3+}$  or  $\text{V}^{4+}$  cations. Examples for low-dimensional  $3d^1$  systems that have attracted special attention are the intriguing Mott insulators  $\text{TiOX}$  ( $X=\text{Cl}, \text{Br}$ ). These compounds crystallize in the  $\text{FeOCl}$ -type structure, consisting of  $\text{Ti} - \text{O} - \text{X}$  layers which are connected by van der Waals forces. The magnetic susceptibility e.g. of  $\text{TiOCl}$  reveals several unusual features, which led to the early proposal that  $\text{TiOCl}$  may be a manifestation of a resonating valence-bond solid. Subsequently, Seidel *et al.* demonstrated that the high temperature susceptibility fits very well to a  $S=1/2$  Heisenberg chain model with nearest-neighbor (NN) antiferromagnetic (AFM) spin-exchange (SE) interaction of  $\sim 660$  K. In view of these findings and electronic structure calculations, it was concluded that  $\text{TiOCl}$  is an example of a Heisenberg chain that undergoes a spin-Peierls transition at 67 K.

Here, we report the magnetic and structural properties of  $\text{TiPO}_4$ [1].  $\text{TiPO}_4$  contains  $\text{Ti}^{3+}$  cations, and we found that  $\text{TiPO}_4$  displays two magneto-structural phase transitions reminiscent of those in the  $\text{TiOX}$  system. In contrast to  $\text{TiOCl}$ , however,  $\text{TiPO}_4$  is a structurally well-defined one-dimensional compound.  $\text{TiPO}_4$  crystallizes in the  $\text{CrVO}_4$  structure-type (SG:  $Cmcm$ ) (see inset in Fig. 1). The  $\text{Ti}^{3+}$  ions, carrying  $S=1/2$  entities, are located in axially compressed  $\text{TiO}_6$  octahedra which share their edges to form corrugated  $\text{TiO}_4$  ribbon chains along the  $c$ -axis. The  $\text{TiO}_4$  ribbon chains are interconnected by sharing corners with distorted  $\text{PO}_4$  tetrahedra[2].

The crystal structure of a very high quality single crystal of  $\text{TiPO}_4$  was re-determined by x-ray single crystal diffraction measurements at various temperatures between 293 K and 90 K. Down to 90 K the structure was found to be identical to that reported by Glaum *et al.*, except for small changes of the lattice parameters and the general atom positions.[2] Upon cooling there is a gradual migration of the density away from the bisecting position into the interstitial position within the ribbon chains. This change is complemented by a reduction of the distance in the  $\text{Ti} - \text{O} - \text{Ti}$ , NN super-exchange pathway, and an increase of the intrachain  $\text{O} - \text{Ti} - \text{O}$  angle. Evidence for a structural change was not found in this temperature range, possibly due to the dynamic character of the intermediate phase as observed by NMR (see below).

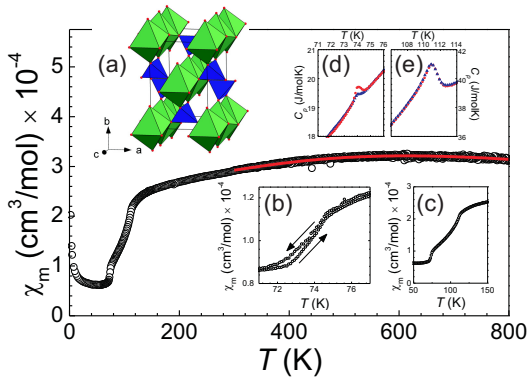


Figure 1: Molar magnetic susceptibility,  $\chi_m(T)$ , of  $\text{TiPO}_4$  measured in a field of 1 T. The (red) line is a fit to a Heisenberg chain with uniform NN AFM SE interaction, see text. Insets: (a) Crystal structure of  $\text{TiPO}_4$ , where green and blue polyhedral represent the  $\text{TiO}_6$  octahedra and  $\text{PO}_4$  tetrahedra, respectively. (b, c)  $\chi_m$  in the region of the phase transitions. (d, e) Heat capacity,  $C_p(T)$ , in the region of the anomalies, where the red circles and blue triangles refer to the heating and cooling data, respectively.

At high temperature the magnetic susceptibility of a polycrystalline sample (Fig. 1, main panel) is characterized by a broad maximum centered at  $\sim 625$  K, indicating short range AFM correlations. After correction for a temperature independent offset to the susceptibility arising from diamagnetic contributions of the closed shells and van Vleck terms, the high temperature magnetic susceptibility can be described very well by a  $S=1/2$  Heisenberg chain with a uniform NN AFM SE interaction of  $965(10)$  K and a  $g$ -factor of  $1.94(3)$ .

Below  $\sim 120$  K the susceptibility reveals two subsequent magnetic phase transitions, indicated by two rapid drops of the susceptibility at  $111(1)$  K and  $74(0.5)$  K. Finally, at lowest temperatures the susceptibility levels off to a value of  $75(10) \times 10^{-6}$   $\text{cm}^3/\text{mol}$ . At very low temperature a slight increase is seen, which we ascribe to a

Curie tail due to  $\sim 70$  ppm of a free  $S=1/2$  spin entities. The anomaly at 74 K shows a thermal hysteresis with a temperature difference of  $\sim 50$  mK between the heating and cooling traces while heating/cooling cycles gave identical susceptibilities for the 111 K anomaly (see Fig. 1 inset (b, c)).

Heat capacities collected on crystals exhibit two  $\lambda$ -type anomalies at 110.9(0.6) K and 74.1(0.3) K, with the lower temperature anomaly also showing a thermal hysteresis, while again no hysteresis is seen for the higher temperature anomaly (see Fig. 1 inset (d, e)). Angular and temperature dependent Electron Spin Resonance measurements (ESR) on single crystals revealed a single Lorentzian resonance line ( $g$ -factor 1.93 - 1.95) and a linewidth decreasing linearly with temperature ( $50 \text{ Oe} \leq \text{FWHM} \leq 300 \text{ Oe}$ ). The integrated intensity of the ESR line mimics the temperature dependence of the magnetic susceptibility and drops to zero below 74 K.

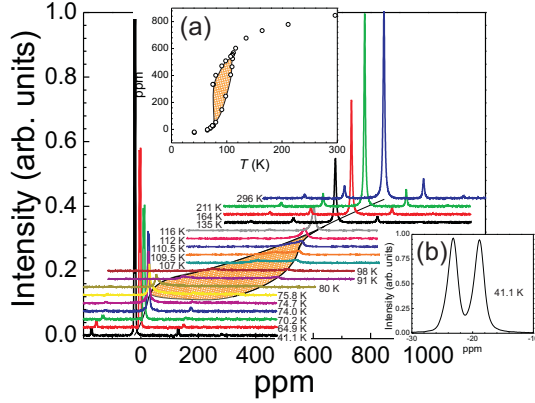


Figure 2: Magic-angle spinning low-temperature  $^{31}\text{P}$  NMR spectra of  $\text{TiPO}_4$  (temperatures indicated). The (orange) hashed area marks the incommensurate continuum. Insets: (a) Peak positions and/or boundary edges versus temperature. (b) Spectrum collected at 41.1 K.

Magic-angle spinning  $^{31}\text{P}$  nuclear magnetic resonance (NMR) spectra were collected on a polycrystalline sample between  $\sim 35$  K and RT reveal apparent similarities between  $\text{TiPO}_4$  and  $\text{TiOX}$ . The spectra are displayed versus temperature in the main panel of Fig. 3. Above  $\sim 140$  K we observe a single  $^{31}\text{P}$  symmetric NMR line accompanied by two sets of very weak symmetrically placed spinning sidebands. Near 116 K the line becomes asymmetric and below 111 K it broadens into an asymmetric continuum limited by two boundary peaks. With decreasing temperature the continuum expands and its intensity decreases. Towards  $\sim 76$  K the continuum finally washes out, whereupon its lower boundary grows into two symmetric lines indicative of two different P atom environments (see inset Fig. 2 (b)). These observations prove a non-magnetic ground state with two distinct P atomic environments, as evidenced especially by the low temperature spectra. The chemical shifts of the  $^{31}\text{P}$  lines amount to  $\sim -20$  ppm in good agreement with what has been found for other diamagnetic orthophosphates, proving the non-magnetic character of the ground state of  $\text{TiPO}_4$ . We ascribe the 74 K phase transition in  $\text{TiPO}_4$  to a spin-Peierls transition with the Ti ... Ti bond alternation within the Ti chains.

To probe the SE interactions of  $\text{TiPO}_4$  we performed a mapping analysis based on the results of density functional calculations. In our analysis we consider the NN and next-nearest neighbor (NNN) intrachain SE interactions  $J_1$  and  $J_2$ , respectively, as well as the interchain SE interaction  $J_3$  (see Fig. 3).

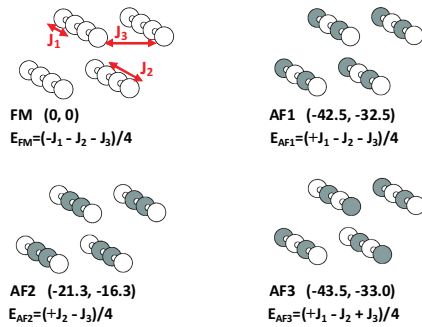


Figure 3: The four ordered spin configurations, FM, AF1, AF2 and AF3, used to extract the values of  $J_1$ ,  $J_2$  and  $J_3$ , where only the  $\text{Ti}^{3+}$  ions are shown for simplicity. The up- and down-spin  $\text{Ti}^{3+}$  sites are indicated by different colors. The numbers in parentheses (from left to right) represent the relative energies in meV per four formula units obtained from GGA+ $U$  calculations with  $U_{\text{eff}} = 2$  and 3 eV, respectively. The expressions of the total SE energy per four formula units are also given.

To evaluate  $J_1 - J_3$ , we determine the relative energies of the four ordered spin states, FM, AF1, AF2, and AF3, shown in Fig. 3, by density functional theory (DFT) electronic band structure calculations employing the Vienna *ab initio* simulation package with the projected augmented-wave method, the generalized gradient

approximation (GGA) for the exchange and the correlation functional. To account for the electron correlation associated to the Ti  $3d$  state, we performed GGA plus onsite repulsion (GGA+ $U$ ) calculations with an effective  $U_{\text{eff}} = U - J = 2$  eV and 3 eV on Ti. The relative energies, per four formula units, of the four ordered spin states are summarized in Fig. 3.

The total SE energies of the four ordered spin states can be expressed in terms of a Heisenberg spin Hamiltonian,  $H = -\sum J_{ij} \vec{S}_i \vec{S}_j$ , where  $J_{ij}$  is the SE interaction between the spins  $\vec{S}_i$  and  $\vec{S}_j$  on the spin sites  $i$  and  $j$ , respectively. By applying the energy expressions obtained for spin dimers with  $N$  unpaired spins per spin site (in the present case,  $N = 1$ ), the total SE energies for the four configurations, per four formula units, are given in Fig. 3. Thus, by mapping the relative energies of the four ordered spin configurations given in terms of the SE parameters (see Fig. 3) onto the corresponding relative energies obtained from the GGA+ $U$  calculations, we obtained the values for the SE parameters  $J_1 - J_3$  (see Table 1). The results of our DFT calculations are in very good quantitative agreement with our experimental findings especially indicating a very large NN intrachain AFM SE interaction. The NNN intrachain SE interaction is almost two orders of magnitude smaller, the interchain interaction  $J_3$  amounts to 2% of  $J_1$ .

Table 1: Values of the SE parameters  $J_1 - J_3$  derived from the mapping analysis (in K).

$J_i$	$U = 2\text{eV}$	$U = 3\text{eV}$
$J_1$	-988	-751
$J_2$	-1.4	+0.7
$J_3$	-20	-15

In order to investigate the origin of the low temperature phase transition and to trace the low temperature crystal structure we considered subgroups of the room-temperature space group  $Cmcm$  and performed a structure optimization using as starting sets those of the subgroups  $Amm2$  and  $Pmnm$ . The lowest-energy structure found was obtained by relaxing the atom positions to relax freely starting from the  $Pmnm$  initial setting, and was lower in energy by  $\sim 48$  meV per formula unit than was the  $Cmcm$  structure. Relaxation from the  $Pmnm$  initial setting reveals a dimerization in the Ti chains with alternating Ti...Ti distances of  $\sim 2.9$  and  $\sim 3.5$  Å, which is comparable in magnitude to that observed in TiOCl. This structure also has two different environments for the P atoms within the  $\text{PO}_4$  units, consistent with our magic-angle spinning NMR spectra.

In conclusion,  $\text{TiPO}_4$  represents a new and exceptional one-dimensional quantum antiferromagnet which exhibits an unusual ground state that is reached via two phase transitions. Our magnetic susceptibility, heat capacity, ESR and  $^{31}\text{P}$  magic-angle spinning NMR measurements supported by our density functional calculations show that  $\text{TiPO}_4$  undergoes a spin-Peierls transition at 74.1(0.3) K, which is preceded by an incommensurate phase extending up to  $\sim 111$  K. The thermal hysteretic behavior of these transitions is consistent with the pattern of discontinuous and continuous transitions seen for TiOCl and TiOBr. At high temperatures the magnetic susceptibility of  $\text{TiPO}_4$  is described by a  $S=1/2$  Heisenberg antiferromagnetic chain with an unprecedented NN SE of  $\sim 1000$  K.

#### References:

- [1] Law, J.M. C. Hoch, R. Glaum, I. Heinmaa, R. Stern, J. Kang, C. Lee, M.-H. Whangbo Phys. Rev. B **83**, 180414(R) (2011).
- [2] Glaum, R. and R. Gruehn. Z. Kristallogr. **198**, 41–47 (1992).

#### In collaboration with:

R. Glaum (Universität Bonn)  
R. Stern and I. Heinmaa (National Institute of Chemical Physics And Biophysics, Tallinn)  
J. Kang, C. Lee, and M.H. Whangbo (North Carolina State University, Raleigh, N.C.)